Electrochemical characterization of platinum nanoparticles prepared in water-in-oil microemulsion in the presence of different modifiers and metal precursors

Roberto A. Martínez-Rodríguez[a,b], Francisco J. Vidal-Iglesias[a], José Solla-Gullón[a], Carlos R. Cabrera[b] and Juan M. Feliu*[a]

Abstract: In this manuscript, Pt nanoparticles have been synthesized using water-in-oil microemulsions in the presence of different modifiers and metal precursors to obtain preferentially oriented nanoparticles. Preferentially oriented cubic nanoparticles, enriched in (100) sites, were mainly prepared for specific concentrations of HCl, HBr, H_2SO_4 and H_3PO_4. On the other hand, citric and oxalic acids increased the amount of (111) sites, although not significantly. Nanoparticles have been electrochemically characterised by hydrogen and Ge ads/desorption processes as well as CO stripping. Finally, the electrocatalytic activity of the nanoparticles having the highest (100) percentage was evaluated towards ammonia oxidation confirming the electrochemical characterization results. The results obtained indicate that, 15% HCl-modified Pt nanoparticles using K_2PtCl_4 as metal precursor displayed the highest amount of (100) sites, 46.7%, and gave the highest peak current density for ammonia oxidation, around 5 times that of a polyoriented Pt.

Introduction

The interest towards the synthesis of shape-controlled metallic nanoparticles has rapidly increased over the last years due to their particular properties. Concerning their catalytic and electrocatalytic properties, the control over the shape directs the orientation of the atoms at the surface of the nanoparticles, and thus, the electrocatalytic activity towards many electrocatalytic reactions which are structure sensitive reactions, can be conveniently tuned [1].

In Electrocatalysis, one of the most studied metals is platinum (Pt) due to its interesting catalytic properties over many electrochemical reactions of high interest such as carbon monoxide [2], ammonia [3], methanol [4], ethanol [4c, 5] or formic acid [4b, 6] oxidations and oxygen [7] or nitrite [8] reductions. Interestingly, all of these electrochemical reactions are structure sensitive. Therefore, by controlling the shape of the nanoparticle and thus, their surface structure, remarkable improvements have been reported for carbon monoxide [2b, 2c, 9], ammonia [9-10] or methanol [4b, 11] oxidations and oxygen reduction [7a] among others. In the particular case of the ammonia oxidation in alkaline medium, Pt nanocubes, ideally enclosed by 6 (100) faces, have shown higher catalytic activity over other kind of Pt nanostructures. This behavior is due to the structure sensitivity to (100) surface planes on which the ammonia oxidation process occurs preferentially [3a, 3b].

The importance of the control over the shape of the nanoparticles has made that a wide variety of methods have been reported to synthesize metallic nanoparticles with well-defined structures. For Pt, there is a plethora of shapes that had been obtained, such as cubes [10b, 10c, 12], tetrahedra [12b] or octahedra [12a] among many others. However, most of these methods require complicated protocols, the need of heat or the use of hazardous materials, making them difficult to be scaled up. From an industrial point of view, synthesis protocols for electrocatalysts' mass production have to fulfill several requirements, so these have to be fast and easy while, if possible, avoiding the need of heating and of expensive reagents.

In a recent communication, we reported a new methodology to prepare cubic Pt nanoparticles with a high yield using a water-in-oil (w/o) microemulsion method [10c]. The formation of the cubic Pt nanoparticles was achieved by adding HCl in the aqueous phase of the w/o microemulsion. In that work, a high concentration of HCl was the key point to modify the shape/surface structure of the nanoparticles. Interestingly a volcano-shaped curve was obtained when correlating the quality of the cubic shape and the amount of HCl, being a 25% HCl the optimum concentration. In a similar way, Pt cubes were also obtained by controlling the amount of H_2SO_4 added as modifier to the aqueous phase of the w/o microemulsion [10b]. In this latter case, the mean size of the Pt cubes was relative smaller than that of the Pt nanocubes synthesized using HCl as surface modifier. Both methods confirmed that HCl and H_2SO_4 act as surface modifiers and had a control over the surface structure when added in the aqueous phase of the w/o microemulsion. Conversely to other synthesis protocols these do fulfill the above mentioned requirements to be scaled up and applied in industry.

On the other hand, cyclic voltammetry is a powerful tool to characterize the surface orientation of platinum surfaces [13]. For this metal, a voltammogram in H_2SO_4 provides direct qualitative information about the surface structure. It is important to recall that it is the surface structure what determines the resulting catalytic activity. In addition some electrochemical reactions such as Bi and Ge irreversible adsorptions can be used to measure the amount of sites from nanoparticles with an orientation (111) and (100), respectively, based on previous calibrations performed with

[a] Mr. R.A. Martínez-Rodríguez, Dr. F.J. Vidal-Iglesias, Dr. J. Solla-Gullón, Prof. J.M. Feliu
Institute of Electrochemistry
University of Alicante
Ap. 99, 03080 Alicante (Spain)
E-mail: juan.feliu@ua.es

[b] Prof. C.R. Cabrera
NASA-URC Center for Advanced Nanoscale Materials (CANM), Department of Chemistry
University of Puerto Rico, Río Piedras Campus
P.O. Box 23346, San Juan 00931-3346, Puerto Rico

well-defined surfaces (single crystals) [13]. Unlike Transmission Electron Microscopy (TEM) where only a small number of nanoparticles are studied, cyclic voltammetry provides representative information of the sample. Additionally, it is worth noting that shape is only an indicator of the surface structure but the surface of a nanoparticle can be perturbed without noticing a difference in a regular TEM image [14]. Interestingly, advanced microscopic techniques such as spherical-aberration-corrected transmission electron microscopy, can be used to provide atomic-resolution information about the local topologies of active sites [15]. Unfortunately, this type of analysis is still quite unusual, very time consuming, again statistically unrepresentative as a limited number of nanoparticles is analysed and obviously, requires very expensive instrumentation not easily available.

The present manuscript extends the study of the effect of the presence of different surface modifiers towards the synthesis of shaped Pt nanoparticles, mainly cubes, also covering the effect of using different metal precursors. In all cases, the surface modifiers have been incorporated to the water phase of the w/o microemulsion. The synthesized Pt nanoparticles have been characterized by TEM and also electrochemically using the so-called hydrogen adsorption/desorption process and germanium irreversible adsorption to quantify the amount of (100) sites. CO stripping and ammonia electrooxidations have been also studied as test reactions in order to determine the catalytic activity.

Results and Discussion

As previously indicated in the introduction, we recently reported the synthesis of Pt nanocubes with a very high yield by adding HCl into the aqueous phase of the w/o microemulsion. In that manuscript the concentration of HCl used ranged from 0 to 37 % and the optimum for the preparation of those shaped nanoparticles was located at 25 %. Nevertheless, the effect of other hydrogen halides was not evaluated. Thus, first of all, the effect on the shape of the Pt nanoparticles using HBr and HI has been also evaluated.

The first modifier to be evaluated was bromhydric acid. HBr has been previously reported to selectively adsorb onto {100} facets of Pd nanocrystals [16]. This selective adsorption stabilizes these facets during the growth of the nanoparticles and then Pd nanocubes, which are enclosed by six {100} facets, are obtained [17]. Figure 1A shows a collection of the positive scans of the CV response for Pt nanoparticles prepared with different concentrations of HBr in the water phase of the w/o microemulsion. As usual, the voltammetric profile of a platinum surface in a 0.5 M H_2SO_4 solution gives us significant information concerning the nature and quantity of the different surface sites. In brief, four different contributions can be observed. These are centred approximately at 0.12, 0.27, 0.37 and 0.53 V vs RHE and are ascribed to the presence of (110) sites, (100) steps and terrace borders, (100) terraces and wide (100) domains and (111) sites, respectively. As it is observed, when increasing the HBr concentration from 0 to 25 %, the contribution due to the (100) terraces remarkably increases, together with the band at 0.27 V due to (100) steps and terrace borders. In general terms, the increase of both (100)-related contributions comes together with a decrease in the (110) contribution, as well as that due to the (111) sites, although this latter signal is very weak in all cases. Interestingly, as in the case of HCl as modifier, the maximum for (100) sites is also observed at 25%. After this maximum is reached, increasing amounts of HBr cause a sudden decrease in the (100) terrace contribution, but not in that due to (100) small sites, which grows even more, unlike the behaviour previously reported when using HCl [10c]. In addition, the other two contributions, related to (110) and (111) sites, also grow.

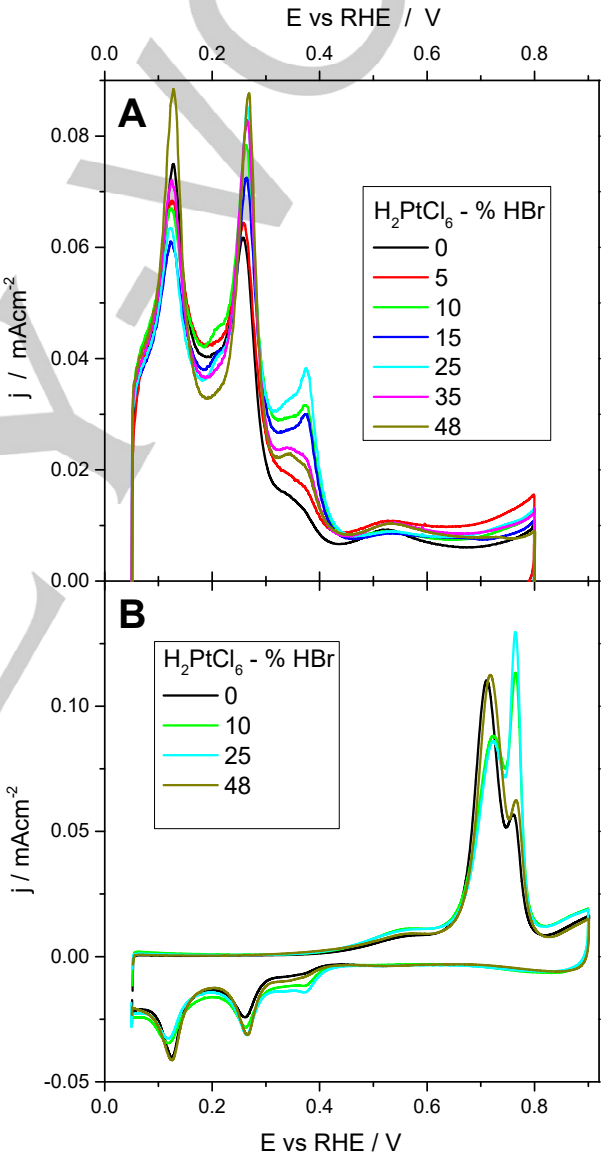

Figure 1. (A) Voltammetric profiles of Pt nanoparticles synthesized using different concentration of HBr in the water phase of w/o microemulsions. Scan rate 50 mV s^{-1}. (B) CO monolayer oxidation. Scan rate 20 mV s^{-1}. Test solution 0.5 M H_2SO_4.

Figure 1B shows the CO stripping oxidation in H_2SO_4 for the samples prepared in the presence of HBr. For sake of clarity, only the voltammetric behaviour of some samples is shown. CO stripping is also a structure sensitive reaction, and it has been previously reported the different voltammetric behaviour of different nanoparticles with different surface structures [2c]. In the voltammograms shown in figure 1B, two different peaks are observed for its oxidation, being centred at 0.73 and 0.78 V, being the latter ascribed to the presence of preferential (100) domains [2c]. In this way the trend observed for the (100) terrace contribution centred at 0.37 V in H_2SO_4 (fig. 1a) is reflected for this CO contribution, increasing from 0 to 25 % and then decreasing for higher HBr concentrations in the water phase. Evidently, the increase of the sharp peak is compensated with a decrease of the other voltammetric feature and vice versa.

In this regard, S.G. Sun's group has recently reported that, in the presence of 1 mM HBr, the potential at which the surface oxidation of a Pt(100) surface starts is shifted to more positive potentials (from 0.6 to 0.9 V vs RHE [18]) thus reflecting a strong bromide-Pt(100) interaction and concluded that the origin of protecting the long-range ordered (100) structure by HBr is mainly through the inhibition of oxygen adsorption. The conclusions from that manuscript clearly agree with our finding. Thus, during the growth of the nanoparticles, bromide is adsorbed on the (100) surfaces thus inducing the preferential formation of nanocubes.

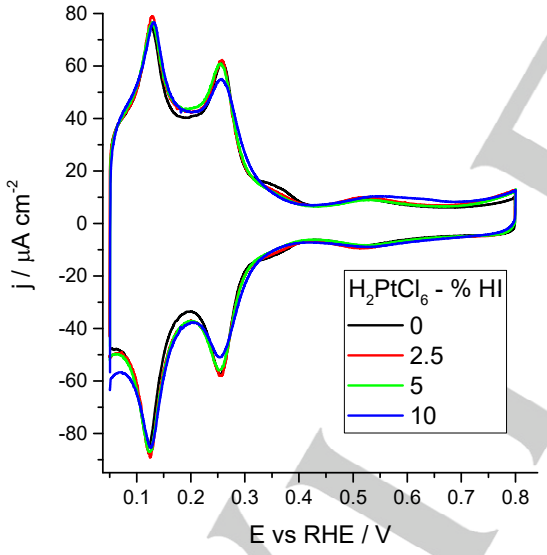

Figure 2. Voltammetric profiles of Pt nanoparticles synthesized using different concentration of HI in the water phase of w/o microemulsions. Scan rate 50 mV s^{-1}. Test solution 0.5 M H_2SO_4.

With the same objective, the effect of the addition of different concentrations of HI up to 10% w/w has been also explored. However, for 10% or higher HI amounts, the platinum precursor was not completely reduced while working in the same experimental conditions as those used throughout the manuscript for all the syntheses. Figure 2 shows the voltammograms in H_2SO_4 of the nanoparticles prepared in the absence and presence of HI in the water phase of the microemulsion. The voltammetric profiles indicate a clear diminution of both (100) step and terrace contributions with increasing amounts of HI. In this case, the lower concentration has been reduced to 2.5 %, giving similar results in comparison with the 5 % and 10 %. In fact, the voltammograms recorded for the 3 types of nanoparticles prepared in the presence of HI show the typical profile of a polyoriented platinum surface. Although much lower concentrations have been used for HI in comparison with HCl or HBr, the results are nevertheless very clear concerning the lack of any preferential orientation. For both HCl and HBr the preferential (100) orientation is very similar and it is also quite clear for a 10 % of the corresponding hydrogen halide, conversely to the effect of HI.

In the case of palladium, the use of KBr into a polyol system led to the formation of nanocubes and nanobars (enclosed by {100} facets) while the use of KCl had a different effect, cuboctahedra being mainly formed [19]. However, the use of KI resulted in much smaller nanoparticles with poorly defined shape due to the much stronger chemisorption of I^- on the nanocrystal surface, being the adsorption strength order $Cl^- < Br^- < I^-$ [20]. This result is similar to that observed in our case for platinum nanoparticles. In the case of HI-modified platinum nanoparticles, the mean size is around 5 nm, while in the case when HCl or H_2SO_4 is used as surface modifier, the mean size is significantly higher (about 12-14 nm [10c] and 9 [10b] nm, respectively). Thus, probably I^- adsorbs very strongly on all the different orientations and consequently no preferential orientation is observed, which may also explain the smaller size of the nanoparticles prepared in the presence of HI.

Besides using hydrogen halides as surface modifiers, H_2SO_4 was also reported to cause a preferential (100) orientation in the synthesized nanoparticles [10b], similarly to that shown for HCl and HBr. In this contribution, a different multiprotic acid was used, but reducing considerably the strength of the acid to analyses its possible effect on the resulting shape/surface structure of the nanoparticles. For this purpose, phosphoric acid was employed. The purity of this acid was 85 % and micellar solution showed good stability and both metal precursor dissolution and chemical reduction reaction could be effectively achieved even at that high acid concentration. The results obtained, figure 3, show a polyoriented profile for the nanoparticles prepared in the absence of modifier (0 % H_3PO_4) which evolves to a slightly preferential (111) voltammogram for increasing H_3PO_4 contents up to a 10 %. Thus, the contribution at 0.51 V is maximum at the expense of the two (100) contributions, which diminish. The (110) contribution becomes also lower, but so slightly that its change can be neglected. Nevertheless, if the phosphoric acid concentration is further increased, the (100) signals become progressively more intense up to the maximum H_3PO_4 concentration in the water phase, thus showing a clear voltammetric behaviour of preferentially oriented (100) nanoparticles. Together with this (100) increase, from the 10 % to the 85 % H_3PO_4, the (110) and (111) contributions diminish.

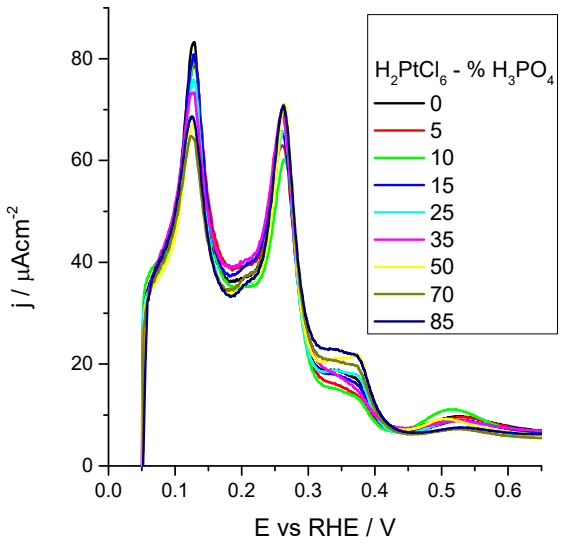

Figure 3. Voltammetric profiles of Pt nanoparticles synthesized using different concentration of H_3PO_4 in the water phase of w/o microemulsions. Scan rate 50 mV s^{-1}. Test solution 0.5 M H_2SO_4.

Important contributions have been also published in the last years concerning the use of different organic molecules to guide metal crystals to a preferential nanoparticle shape. For example, Chiu et al. reported the preparation of platinum nanoparticles using many different modifiers such as ascorbic acid, catechol, hydroquinone, syringol or resorcinol among others [21]. The authors concluded that negative electrostatic potential on the aromatic ring is prerequisite to display binding selectivity to Pt(111), while a neutral to positive one prefers Pt(100). In addition, they claimed that the geometric matching between molecular binding sites and surface lattices plays a role as well in facet selectivity. In addition, Ruan et al. recently studied the synthesis of platinum nanoparticles in the presence of different peptides [22]. They observed that those with phenylalanine gave high tetrahedral yields. Similarly but for Pd, Lim et al. reported that citrate or citric acid could selectively stabilize {111} facets and thus, favour the formation of Pd nanocrystals enclosed by {111} facets, such as octahedrons [23].

Accordingly, we have evaluated some organic acids at certain concentrations in order to evaluate their effect as surface modifiers. The selection of citric, oxalic and ascorbic acids as modifiers has been made due to the fact that those are well known in the case of Pd for the synthesis of octahedra and cubes [24]. The percentages used for citric acid, ascorbic acid and oxalic acid have been 9, 8 and 4% respectively. These values are in the range of those used in bibliography [23]. The other parameters of synthesis have been the same as in previous experiments.

Figure 4 shows the voltammograms recorded for the different nanoparticles modified with those organic acids. The effect of these modifiers is very small, but as in the case of Pd [23] they cause a moderate increase in the amount of (111) sites, although to a much lower extent. This (111)-site growth comes together with a diminution of the (100)-terrace contribution. The maximum increase of (111) sites is recorded for citric acid, which is in agreement with molecular dynamics simulations performed for Pd, for which the strong interaction of the OH functional group in the citric acid molecule with the Pd(111) surface, explains why nanoparticles synthesized in its presence are dominated by (111) facets [25].

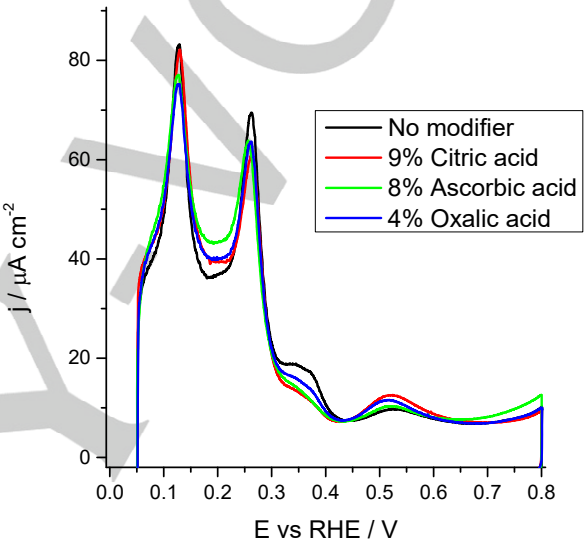

Figure 4. Voltammetric profiles of Pt nanoparticles synthesized using three different organic acids in the water phase of w/o microemulsions. Scan rate 50 mV s^{-1}. Test solution 0.5 M H_2SO_4.

The nanoparticles prepared up to this point as well as those previously reported with this methodology [10b, 10c] have been synthesised using H_2PtCl_6 as metal precursor. Consequently, the effect of using a different platinum source has also been analysed. This synthesis was exclusively performed with those modifiers which gave the most satisfactory results with H_2PtCl_6 as platinum precursor. Thus, nanoparticles were synthesized using K_2PtCl_4 as platinum source in the presence of different concentrations of HCl and H_2SO_4, being their electrochemical characterization shown in figures 5 and 6, respectively. Figure 5A shows the voltammetric profiles in 0.5 M H_2SO_4 of the Pt nanoparticles synthesized using HCl as surface modifier up to a maximum concentration of 20%. An impressive change in the so called hydrogen region is clearly observed when the amount of HCl used in the synthesis is increased (for sake of comparison, the voltammetric profile of the nanoparticles synthesized with K_2PtCl_4 in the absence of HCl is also plotted). The relative increase of the peaks at 0.27 and especially at 0.37 V vs RHE denotes a clear change in the surface structure produced by the addition of HCl up to a 15%. Those two contributions (related to (100) Pt steps and terraces and wide

domains) remarkably increase with the HCl concentration up to that 15%. The increase of (100) sites up to that optimum 15% is counterbalanced with the diminution of the (110) and (111) signals, although the latter is considerable weaker. For higher HCl amounts (20% HCl), the (100) quality is drastically affected. Thus, for the sample prepared in the presence of a 20% HCl, the peaks corresponding to the (100) contributions decrease in intensity while the (110)-site related signal increases, thus confirming the loss of quality concerning the (100) preferential orientation. It is important to highlight that the (100) quality of the 15% HCl-modified Pt nanoparticles is significantly better that that previously obtained in the presence of 25% HCl using H_2PtCl_6 as platinum precursor [10c] and with a significant lower amount of surface modifier.

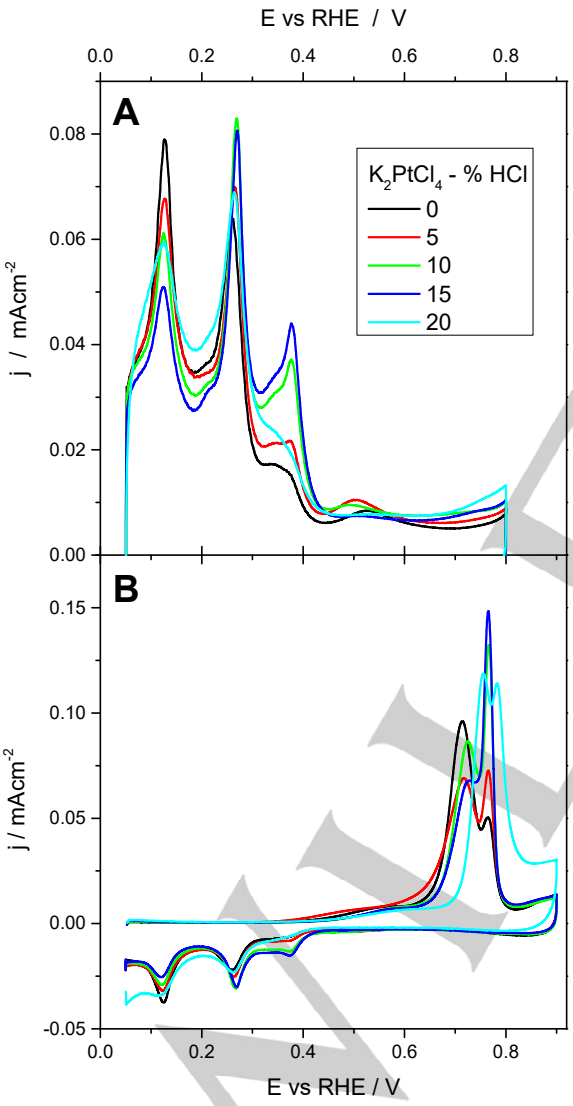

Figure 5. (A) Voltammetric profiles of the Pt nanoparticles using K_2PtCl_4 as Pt precursor in the presence of different HCl percentages. Scan rate 50 mVs^{-1}. (B) CO monolayer oxidation. Scan rate 20 mVs^{-1}. Test solution 0.5 M H_2SO_4.

Similarly, the CO stripping on these nanoparticles (showed in Figure 5B) although less sensitive, also confirms those previous results. The relative decrease of the peak centered at 0.73 V and the consecutive increase of the sharp peak at 0.78 V vs RHE clearly highlights the increase of the Pt (100) terraces sites and wide domains for the samples prepared using K_2PtCl_4 as platinum source and with HCl up to 15%.

The use of H_2SO_4 as surface modifier also denotes a relative change in the surface structure of the Pt nanoparticles using K_2PtCl_4 as Pt precursor (figure 6). Previous results for H_2SO_4-modified Pt nanoparticles using H_2PtCl_6 as modifier showed that the synthesis was very sensitive to the amount of modifier added, and that the amount of (100) sites progressively grows with the acid concentration. The maximum was obtained for a 25% (in volume) H_2SO_4, which corresponds to a 38% w/w, before the system became unstable. In the case of using K_2PtCl_4 as metal precursor, a 50 % H_2SO_4 could be reached, being the quality of the sample in relation to the amount of (100) sites very similar for both metal precursors at the best mentioned concentrations, as shown in figure 6A and reference [10b]). Figure 6B shows the CO monolayer stripping voltammograms for which the growth of the two (100) signals in figure 6A can be followed with the second CO oxidation peak, which is centered at 0.75 V.

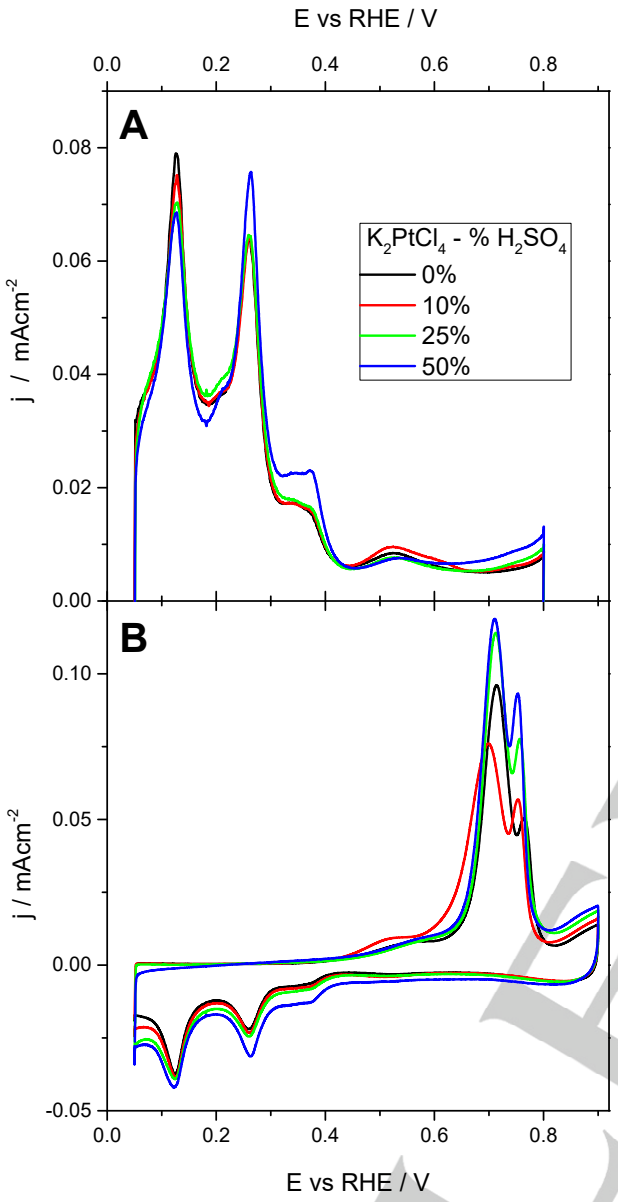

Figure 6. (A) Voltammetric profile of the Pt nanoparticles synthesized using H_2SO_4 at different concentrations. Scan rate 50 mVs^{-1}. (B) CO monolayer oxidation at 20 mVs^{-1}. Test solution 0.5 M H_2SO_4.

So far we have qualitatively analysed the amount of (100) sites. Nevertheless, the amount of this type of site can be conveniently quantitatively measured through germanium irreversible adsorption as described in previous contributions [13, 26]. Briefly, the glassy carbon electrode with the platinum nanoparticles attached was transferred with a drop of a 10^{-2} M GeO_2 and 1 M NaOH solution into an electrochemical cell with 0.5 M H_2SO_4. The contact with the solution was performed at controlled potential, 0.1 V vs RHE. From the voltammogram obtained, the area due to the germanium contribution was obtained by integration and from that area, the (100)-site percentage could be obtained by using the calibration expression found in literature, which was obtained with model surfaces (single crystals) [26].

Table 1 presents the values obtained for the quantification of (100) sites, given in percentages, for the most preferentially oriented samples according to their cyclic voltammograms in H_2SO_4. In addition, the data for the HCl and H_2SO_4 modified Pt nanoparticles prepared with H_2PtCl_6 as metal precursor and reported previously [10b, 10c] are also included.

Table 1. Relative percentage of (100) sites measured by Ge irreversible adsorption for different additives in the aqueous phase of water-in-oil microemulsion

Additive	% (100) sites
Metal precursor H_2PtCl_6	
25% HCl	44.0 [10c]
38% H_2SO_4	35.0 [10b]
25% HBr	44.9
85% H_3PO_4	29.2
Metal precursor K_2PtCl_4	
15% HCl	46.7

From the results shown in table 1, it is confirmed that the nanoparticles with the highest amount of (100) sites are those prepared using K_2PtCl_4 as metal precursor and a 15% HCl as surface modifier. This result was somehow expected from the voltammograms in H_2SO_4 shown previously and particularly, from the contribution located at 0.37 V, for which this sample showed the largest and most defined peak. All the samples prepared in the presence of K_2PtCl_4 and HCl were analyzed with this Ge quantification method and a volcano shape curve similar to that reported previously [10c] was obtained when comparing the amount of (100) sites with the HCl percentage. Thus, percentages of 18.6, 19.1, 40.8, 46.7 and 28.9 % sites with (100) geometry were obtained for non-modified and 5, 10, 15 and 20 % HCl with K_2PtCl_4 as metal precursor (result not shown).

In parallel, all samples were also analysed by TEM. Although CV gives a complete behavior of the sample and the response is a direct reflect of all surface sites present at the surface of the nanoparticles, TEM also gives qualitative information concerning the quality of the sample. Thus, samples displaying a high amount of (100) sites are expected to be preferentially cubic, as a cube is ideally enclosed by 6 (100) faces. TEM analysis of the samples was not an easy task. TEM grids were prepared collecting the samples before adding acetone, which causes phase separation and makes the nanoparticles precipitate and then agglomerate. This agglomeration has to be avoided in order to obtain high quality TEM images. Unfortunately, the acids used as surface

modifiers are in such a high concentration in many of the samples that the grid is damaged during the TEM sample preparation. In some of the cases the sample cannot be analyzed due to this problem and in others, small grey dots that look like quasi spherical nanoparticles are clearly observed. EDX experiments confirmed that those grey dots were not platinum.

Figure 7 shows some representative TEM figures obtained for some of the samples of interest. Figure 7A shows the quasi spherical shape of HI-modified nanoparticles synthesized using H_2PtCl_6 as metal precursor. As deduced from the voltammogram CVs shown in figure 2, the presence of HI does not originate any preferential orientation and the mean size is smaller. On the other hand, figures 7B, 7C and 7D show the cubic shapes obtained with 10% HBr and 15% HCl-modified platinum nanoparticles prepared using H_2PtCl_6 and K_2PtCl_4, respectively, as metal precursor. As it is observed, both samples show good quality cubes, but voltammograms shown in figure 1 and figure 5 make clear that the latter are better (100) preferentially oriented. In addition, in figure 7D the previously mentioned problem concerning the sample preparation for acid-rich samples is observed, especially at the top of the image as small grey dots that without any EDX analysis could be taken as much smaller Pt nanoparticles without any preferential orientation. An explanation for the higher amount of (100) terrace sites could be also justified considering the particle size of the nanoparticles. In fact the larger the nanoparticles, the wider can be the (100) surface domains. In fact H_2SO_4 and HCl modified nanoparticles obtained from H_2PtCl_6 and HCl modified nanoparticles from K_2PtCl_4 have a mean particle size of about 9, 12-14 and 17 nm, respectively.

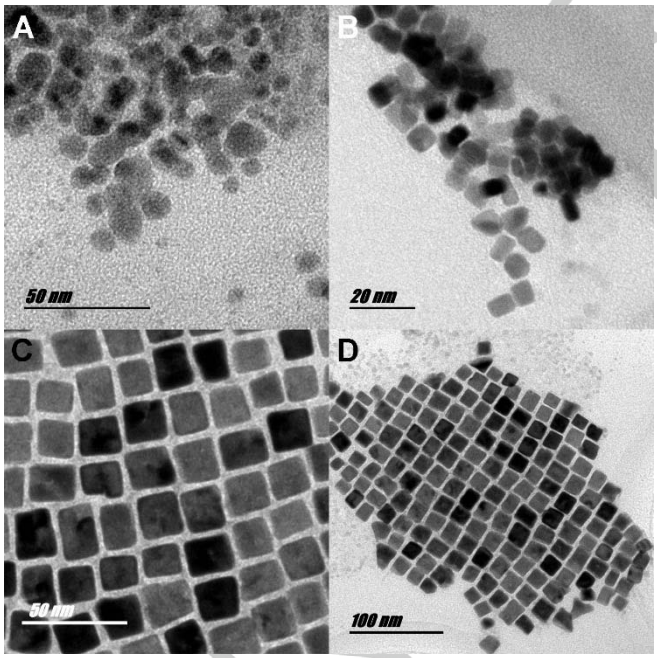

Figure 7. Pt nanoparticles synthesized using w/o microemulsion with H_2PtCl_6 as metal precursor prepared in the presence of (A) 2.5% HI, (B) 10% HBr and (C) and (D) using K_2PtCl_4 as metal precursor with 15% HCl.

The present results point out that we can prepare preferentially oriented cubic nanoparticles with a high yield using some acids as surface modifiers. The importance of preparing this type of catalysts lies in the fact that many electrochemical reactions of high interest are structure sensitive, so these cubic nanoparticles could be chosen as better catalysts for electrochemical reactions in which (100) sites are favorable. Ammonia electrooxidation is one of the most structure sensitive reactions which takes place almost exclusively on (100) sites [3b, 3c]. In fact, this reaction is so sensitive that it can also be used as a tool to get information about the quality and amount of (100) sites [10c]. For this study, the nanoparticles containing a high amount of (100) sites, were used as electrocatalysts and the results are given in figure 8. For sake of comparison, the data corresponding to quasi-spherical nanoparticles (HI modified) which give the lowest current densities, are also shown. As it is observed, the Pt nanoparticles synthesized using K_2PtCl_4 as metal precursor and using a 15% HCl as surface modifier displayed the best catalytic activity for ammonia oxidation in terms of peak current density. This result was expected from the Ge data (table 1), for which this catalyst was the one with the highest (100) percentage. In addition, the data for 25% HBr, 25% HCl and 47% H_2SO_4-modified platinum nanoparticles are also very satisfactory.

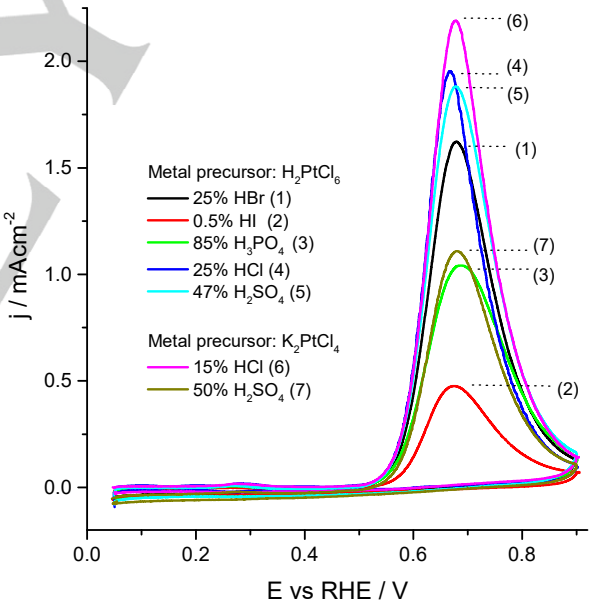

Figure 8. Voltammetric profiles for ammonia electrooxidation for different Pt nanoparticles synthesized using different acid concentrations in the aqueous phase of the w/o microemulsion and different metal precursors. Scan rate 10 mV s^{-1}.Test solution: 0.2 M NaOH + 0.1 M NH_3.

Conclusions

Pt nanoparticles with preferential shapes were synthesized using different acids and using different Pt precursors in water-in-oil microemulsions. On the one hand, the effect of different inorganic acids was analysed. First of all, several hydrogen halides were used. Specifically, HBr and HI were used and compared with the effect of HCl, which had been already studied in a previous publication [10c]. HBr, as in the case of HCl, gave nanoparticles with a high proportion of (100) sites and showed a preferential cubic shape as observed by TEM. On the contrary HI-modified Pt nanoparticles did not show a preferential surface structure and their CV in H_2SO_4 solution is characteristic of a polyoriented surface. In addition, H_2SO_4, had also been used previously as a successful modifier toward the synthesis of preferentially oriented cubic nanoparticles [10b]. In this manuscript, the effect of a weaker multiprotic acid, H_3PO_4, was also evaluated, yielding nanoparticles with a slightly higher percentage of (100) sites than a polyoriented surface but poorer results than in the case of H_2SO_4.

On the other hand, some organic modifiers were used in order to obtain (111)-rich nanoparticles. Similar organic molecules had been successfully used for synthesising (111)-rich palladium nanoparticles, although not in microemulsion. For this purpose citric, ascorbic and oxalic acids were used as modifiers. Although an increase in the number of (111) sites was accomplished, this improvement was quite subtle.

Finally, the nature of the Pt source was also explored. Thus, the metal precursor H_2PtCl_6 used for the previous experiments was replaced by K_2PtCl_4 and employed together with those modifiers giving the best results (HCl and H_2SO_4). Although the latter did not significantly improve the results obtained with the H_2PtCl_6 as metal precursor, HCl yielded very well defined cubic nanoparticles, with the highest (100) percentage among those obtained with this methodology with the different used modifiers. Finally, the nanoparticles having the highest amounts of (100) sites were tested towards ammonia electrooxidation and, as expected, the highest peak current density was obtained with the 15% HCl modified Pt nanoparticles prepared with K_2PtCl_4 as metal precursor.

Experimental Section

Pt nanoparticles were synthesized in a similar methodology to that previously reported [10c], using a w/o microemulsion of water/polyethylene glycol dodecyl ether (Brij®L4, Sigma-Aldrich)/n-heptane (99.86% p.a. from Acros Organics) with a volume percentage of 3, 16.5 and 80.5 %, respectively. In the water phase the metal precursor (constant 0.1 M concentration) together with the surface modifier were added. In this manuscript, two different Pt precursors have been used, H_2PtCl_6 (40% weight Pt Acros Organics) and K_2PtCl_4 (99.99% Acros Organics). The different modifiers that have been used are the following: hydrochloric acid (HCl 37% p.a. from Panreac), sulfuric acid (H_2SO_4 95-97%, p.a. from Merck), bromhydric acid (HBr 48% ACS reagent from Acros Organics), iodhydric acid (HI 57% from Sigma Aldrich) phosphoric acid (H_3PO_4 85%, p.a. from Merck), citric acid (99.7% from Prolabo), ascorbic acid (reagent grade from Sigma-Aldrich) and oxalic acid ($(COOH)_2$ x $2H_2O$ ACS, ISO, Reagent) from Merck. Once the microemulsion was prepared and ultrasonically mixed, $NaBH_4$ (Reagent Plus 99% from Sigma Aldrich) as solid was added as reducing agent. The amount of the reducing agent was that necessary for a 1 M concentration in the water phase. The complete reduction usually takes place in a couple of minutes in the absence of any surface modifier. Nevertheless, in the presence of the modifiers, the process could take up to 8 minutes to make the micellar solution become black. Thirty minutes after the reducing agent was added, acetone was added to the solution to cause phase separation. Once the nanoparticles precipitated, they were washed several times with acetone and ultrapure water (Millipore, 18.2 MΩ cm) in order to remove the modifiers and the surfactant. Finally, the nanoparticles were stored in ultrapure water as a suspension. The concentration of the different modifiers was limited to the as-purchased reagent concentration except when the nature and high acid concentration of the acid cause instability of the micellar solution. For example, in the case of HBr the concentrations varied from 0% (pure water) to 48% (commercial solution). However, for HI the maximum concentration used in the water phase was 10%. Concentrations of the modifiers throughout the manuscript are expressed in w/w %.

Surface characterisation of the nanoparticles was performed by Transmission Electron Microscopy (TEM). TEM allowed the shape and the size distribution of the samples to be estimated. These experiments were performed with a JEOL, JEM-2010, working at 200 kV. Electrochemical measurements were performed using a three-electrode electrochemical cell using a VMP3 multichannel potentiostat (BioLogic) with a NStat configuration (1 counter electrode, 1 reference electrode and up to 8 working electrodes working simultaneously). The counter electrode was a platinum wire and the reference electrode was a reversible hydrogen electrode (RHE) connected to the cell through a Luggin capillary. Gold collector electrodes, on which the nanoparticles were deposited, were used as working electrodes. Before each experiment, the working electrode was mechanically polished with alumina and rinsed with ultra-pure water to eliminate the impurities. After checking the cleanness of the gold surface, a drop (≈ 5 µl) was dropcasted on the surface and dried in an argon atmosphere. The active surface area of the Pt NPs was determined by the charge involved in the so-called hydrogen UPD region (between 0.06 V - 0.6 V) after the substraction of the double layer charging contribution and using the value of 230 µC cm^{-2} [27].

Acknowledgements

This work has been financially supported by the Ministerio de Economía y Competitividad (projects CTQ2013-44083-P and CTQ2013-48280-C3-3-R) and Generalitat Valenciana (project PROMETEOII/2014/013 and Beca Santiago Grisolía).

Keywords: electrocatalysis • microemulsion • nanoparticles • platinum • shape

[1] a) J. Solla-Gullon, F. J. Vidal-Iglesias, J. M. Feliu, *Annu. Rep. Prog. Chem., Sect. C* **2011**, *107*, 263-297; b) M. T. M. Koper, *Nanoscale* **2011**, *3*, 2054-2073; c) F. J. V.-I. J. Solla-Gullón, E. Herrero, J. M. Feliu, A. Aldaz, in *Polymer Electrolyte Fuel Cells: Science, Applications, and Challenges* (Ed.: A. A. Franco), Pan Stanford Publishing Pte Ltd, Boca Raton, Florida, **2013**, pp. 93-52; d) Y. Bing, H. Liu, L. Zhang, D. Ghosh, J. Zhang, *Chem. Soc. Rev.* **2010**, *39*, 2184-2202; e) Z. Peng, H. Yang, *Nano Today* **2009**, *4*, 143-164; f) J. Chen, B. Lim, E. P. Lee, Y. Xia, *Nano Today* **2009**, *4*, 81-95; g) H. You, S. Yang, B. Ding, H. Yang, *Chem. Soc. Rev.* **2013**, *42*, 2880-2904.

[2] a) K. J. J. Mayrhofer, M. Arenz, B. B. Blizanac, V. Stamenkovic, P. N. Ross, N. M. Markovic, *Electrochim. Acta* **2005**, *50*, 5144-5154; b) S. Brimaud, S. Pronier, C. Coutanceau, J. M. Léger, *Electrochem. Commun.* **2008**, *10*, 1703-1707; c) J. Solla-Gullón, F. J. Vidal-Iglesias, E. Herrero, J. M. Feliu, A. Aldaz, *Electrochem. Commun.* **2006**, *8*, 189-194.

[3] a) V. Rosca, M. T. M. Koper, *Phys. Chem. Chem. Phys.* **2006**, *8*, 2513-2524; b) F. J. Vidal-Iglesias, J. Solla-Gullón, V. Montiel, J. M. Feliu, A. Aldaz, *J. Phys. Chem. B* **2005**, *109*, 12914-12919; c) F. J. Vidal-Iglesias, N. Garcia-Araez, V. Montiel, J. M. Feliu, A. Aldaz, *Electrochem. Commun.* **2003**, *5*, 22-26.

[4] a) A. V. Tripkovic, S. L. J. Gojkovic, K. D. Popovic, J. D. Lovic, *J. Serb. Chem. Soc.* **2006**, *71*, 1333-1343; b) J. Solla-Gullón, F. J. Vidal-Iglesias, A. López-Cudero, E. Garnier, J. M. Feliu, A. Aldaz, *Phys. Chem. Chem. Phys.* **2008**, *10*, 3689-3698; c) S. B. Han, Y. J. Song, J. M. Lee, J. Y. Kim, K. W. Park, *Electrochem. Commun.* **2008**, *10*, 1044-1047.

[5] C. Buso-Rogero, V. Grozovski, F. J. Vidal-Iglesias, J. Solla-Gullon, E. Herrero, J. M. Feliu, *J. Mater. Chem. A* **2013**, *1*, 7068-7076.

[6] C. Wang, H. Daimon, Y. Lee, J. Kim, S. Sun, *J. Am. Chem. Soc.* **2007**, *129*, 6974-6975.

[7] a) C. M. Sanchez-Sanchez, J. Solla-Gullon, F. J. Vidal-Iglesias, A. Aldaz, V. Montiel, E. Herrero, *J. Am. Chem. Soc.* **2010**, *132*, 5622-5624; b) A. Wieckowski, *Interfacial electrochemistry : theory, experiment, and applications*, Marcel Dekker, New York, **1999**; c) N. M. Markovic, H. A. Gasteiger, P. N. Ross, *J. Phys. Chem.* **1995**, *99*, 3411-3415; d) A. A. Gewirth, M. S. Thorum, *Inorg. Chem.* **2010**, *49*, 3557-3566; e) R. R. Adzic, in *Electrocatalysis* (Eds.: J. Lipkowski, P. N. Ross), Wiley-VCH, New York, **1998**, pp. 197-242; f) A. M. Gomez-Marin, R. Rizo, J. M. Feliu, *Catal. Sci. Technol.* **2014**, *4*, 1685-1698; g) A. Kuzume, E. Herrero, J. M. Feliu, *J. Electroanal. Chem.* **2007**, *599*, 333-343; h) A. S. Bandarenka, H. A. Hansen, J. Rossmeisl, I. E. L. Stephens, *Phys. Chem. Chem. Phys.* **2014**, *16*, 13625-13629; i) M. D. Maciá, J. M. Campina, E. Herrero, J. M. Feliu, *J. Electroanal. Chem.* **2004**, *564*, 141-150.

[8] a) M. Duca, M. C. Figueiredo, V. Climent, P. Rodriguez, J. M. Feliu, M. T. M. Koper, *J. Am. Chem. Soc.* **2011**, *133*, 10928-10939; b) M. Duca, M. O. Cucarella, P. Rodriguez, M. T. M. Koper, *J. Am. Chem. Soc.* **2010**, *132*, 18042-18044; c) M. Duca, P. Rodriguez, A. I. Yanson, M. T. M. Koper, *Top. Catal.* **2014**, *57*, 255-264.

[9] J. Solla-Gullón, F. J. Vidal-Iglesias, P. Rodríguez, E. Herrero, J. M. Feliu, J. Clavilier, A. Aldaz, *J. Phys. Chem. B* **2004**, *108*, 13573-13575.

[10] a) F. J. Vidal-Iglesias, J. Solla-Gullón, P. Rodríguez, E. Herrero, V. Montiel, J. M. Feliu, A. Aldaz, *Electrochem. Commun.* **2004**, *6*, 1080-1084; b) R. A. Martínez-Rodríguez, F. J. Vidal-Iglesias, J. Solla-Gullón, C. R. Cabrera, J. M. Feliu, *ChemPhysChem* **2014**, *15*, 1997-2001; c) R. A. Martínez-Rodríguez, F. J. Vidal-Iglesias, J. Solla-Gullon, C. R. Cabrera, J. M. Feliu, *J. Am. Chem. Soc.* **2014**, *136*, 1280-1283.

[11] C. Susut, Y. Tong, *Electrocatalysis* **2011**, *2*, 75-81.

[12] a) H. Song, F. Kim, S. Connor, G. A. Somorjai, P. Yang, *J. Phys. Chem. B* **2005**, *109*, 188-193; b) C.-Y. Chiu, Y. Li, L. Ruan, X. Ye, C. B. Murray, Y. Huang, *Nat Chem* **2011**, *3*, 393-399; c) T. S. Ahmadi, Z. L. Wang, T. C. Green, A. Henglein, M. A. El-Sayed, *Science* **1996**, *272*, 1924-1926.

[13] J. Solla-Gullón, P. Rodríguez, E. Herrero, A. Aldaz, J. M. Feliu, *Phys. Chem. Chem. Phys.* **2008**, *10*, 1359-1373.

[14] F. J. Vidal-Iglesias, J. Solla-Gullón, E. Herrero, V. Montiel, A. Aldaz, J. M. Feliu, *Electrochem. Commun.* **2011**, *13*, 502-505.

[15] L. C. Gontard, L. Y. Chang, C. J. D. Hetherington, A. I. Kirkland, D. Ozkaya, R. E. Dunin-Borkowski, *Angew. Chem. Int. Ed.* **2007**, *46*, 3683-3685.

[16] Y. Xiong, H. Cai, B. J. Wiley, J. Wang, M. J. Kim, Y. Xia, *J. Am. Chem. Soc.* **2007**, *129*, 3665-3675.

[17] a) B. Lim, H. Kobayashi, P. H. C. Camargo, L. F. Allard, J. Liu, Y. Xia, *Nano Res.* **2010**, *3*, 180-188; b) M. Jin, H. Liu, H. Zhang, Z. Xie, J. Liu, Y. Xia, *Nano Res.* **2011**, *4*, 83-91.

[18] C.-D. Xu, J.-Y. Ye, L. Chen, D.-H. Chen, J.-T. Li, C.-H. Zhen, S.-G. Sun, *Electrochim. Acta* **2015**, *162*, 129-137.

[19] B. Wu, N. Zheng, *Nano Today* **2013**, *8*, 168-197.

[20] a) M. P. Soriaga, J. A. Schimpf, A. Carrasquillo, J. B. Abreu, W. Temesghen, R. J. Barriga, J. J. Jeng, K. Sashikata, K. Itaya, *Surf. Sci.* **1995**, *335*, 273-280; b) A. Carrasquillo Jr, J.-J. Jeng, R. J. Barriga, W. F. Temesghen, M. P. Soriaga, *Inorg. Chim. Acta* **1997**, *255*, 249-254.

[21] C.-Y. Chiu, H. Wu, Z. Yao, F. Zhou, H. Zhang, V. Ozolins, Y. Huang, *J. Am. Chem. Soc.* **2013**, *135*, 15489-15500.

[22] L. Ruan, H. Ramezani-Dakhel, C.-Y. Chiu, E. Zhu, Y. Li, H. Heinz, Y. Huang, *Nano Lett.* **2013**, *13*, 840-846.

[23] B. Lim, Y. Xiong, Y. Xia, *Angew. Chem. Int. Ed.* **2007**, *46*, 9279-9282.

[24] a) M. Shao, T. Yu, J. H. Odell, M. Jin, Y. Xia, *Chem. Commun.* **2011**, *47*, 6566-6568; b) Y. Xiong, Y. Xia, *Adv. Mater. (Weinheim, Ger.)* **2007**, *19*, 3385-3391; c) B. Lim, M. Jiang, J. Tao, P. H. C. Camargo, Y. Zhu, Y. Xia, *Adv. Funct. Mater.* **2009**, *19*, 189-200.

[25] J. Yue, Z. Du, M. Shao, *Chem. Phys. Lett.* **2016**, *659*, 159-163.

[26] P. Rodríguez, E. Herrero, J. Solla-Gullón, F. J. Vidal-Iglesias, A. Aldaz, J. M. Feliu, *Electrochim. Acta* **2005**, *50*, 3111-3121.

[27] Q. S. Chen, J. Solla-Gullon, S. G. Sun, J. M. Feliu, *Electrochim. Acta* **2010**, *55*, 7982-7994.

Entry for the Table of Contents (Please choose one layout)

Layout 1:

ARTICLE

The electrochemical characterisation of Pt nanoparticles prepared in water-in-oil microemulsions in the presence of different surface modifiers is performed. Well defined cubic nanoparticles with a preferential (100) surface structure are obtained and tested for different electrocatalytic reactions.

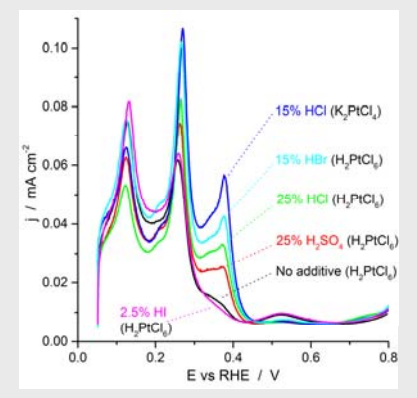

*Roberto A. Martínez-Rodríguez, Francisco J. Vidal-Iglesias, José Solla-Gullón, Carlos R. Cabrera and Juan M. Feliu**

Page No. – Page No.

Electrochemical characterization of platinum nanoparticles prepared in water-in-oil microemulsion in the presence of different modifiers and metal precursors